

# Flow-induced endothelial cell alignment requires the RhoGEF Trio as a scaffold protein to polarize active Rac1 distribution

Jeffrey Kroon<sup>a</sup>, Niels Heemsker<sup>a</sup>, Martin J. T. Kalsbeek<sup>a</sup>, Vivian de Waard<sup>b</sup>, Jos van Rijssel<sup>a</sup>, and Jaap D. van Buul<sup>a,\*</sup>

<sup>a</sup>Department of Plasma Proteins and Department of Molecular Cell Biology, Sanquin Research and Landsteiner Laboratory, Academic Medical Center, University of Amsterdam, Amsterdam 1066 CX, Netherlands; <sup>b</sup>Department of Medical Biochemistry, Academic Medical Center, University of Amsterdam, Amsterdam 1105 AZ, Netherlands

**ABSTRACT** Endothelial cells line the lumen of the vessel wall and are exposed to flow. In linear parts of the vessel, the endothelial cells experience laminar flow, resulting in endothelial cell alignment in the direction of flow, thereby protecting the vessel wall from inflammation and permeability. In order for endothelial cells to align, they undergo rapid remodeling of the actin cytoskeleton by local activation of the small GTPase Rac1. However, it is not clear whether sustained and local activation of Rac1 is required for long-term flow-induced cell alignment. Using a FRET-based DORA Rac1 biosensor, we show that local Rac1 activity remains for 12 h upon long-term flow. Silencing studies show that the RhoGEF Trio is crucial for keeping active Rac1 at the downstream side of the cell and, as a result, for long-term flow-induced cell alignment. Surprisingly, Trio appears to be not involved in flow-induced activation of Rac1. Our data show that flow induces Rac1 activity at the downstream side of the cell in a Trio-dependent manner and that Trio functions as a scaffold protein rather than a functional GEF under long-term flow conditions.

## Monitoring Editor

Manuel Théry  
CEA, Hopital Saint Louis

Received: Jun 13, 2016

Revised: May 5, 2017

Accepted: May 9, 2017

## INTRODUCTION

Endothelial cells (ECs) lining the blood vessels are constantly exposed to shear stress (Ballermann *et al.*, 1998; Hahn and Schwartz, 2009). These frictional forces created by blood flow regulate important pathological and physiological responses, such as arteriogenesis (Galie *et al.*, 2014) and acute vessel tone regulation, and are furthermore involved in atherosclerosis (Tzima *et al.*, 2005; Hahn and Schwartz, 2009; Chiu and Chien, 2011). Atherosclerotic lesions mostly develop near branch points and curvatures of the arterial tree. These regions are characterized by low and disturbed

shear stress patterns, leading to failure in EC elongation and alignment (Chappell *et al.*, 1998; Malek *et al.*, 1999; Chiu and Chien, 2011).

Laminar shear stress, however, observed in linear parts of the arteries, induces the alignment of ECs in the direction of flow, which is accompanied by actin cytoskeleton remodeling (Tzima *et al.*, 2002; Tzima, 2006; Pan, 2009). This high laminar shear stress, ranging from 10 to 70 dynes/cm<sup>2</sup> in the arterial vascular network, is atheroprotective (Malek *et al.*, 1999). Endothelial cells are able to sense flow by several mechanosensing mechanisms. Well-studied examples are ion channels, primary cilia expressed at the apical surface of cells, and the mechanosensing complex comprising PECAM-1, VEGFR-2, and VE-cadherin present at EC–cell junctions (Hoger *et al.*, 2002; Tzima *et al.*, 2005; van der Heiden *et al.*, 2008). These signaling proteins play an important role in transmitting flow-induced physiological force into intracellular signals and are therefore essential for flow-induced alignment.

In order for cells to align in the direction of the flow, they remodel their actin cytoskeleton by regulating small RhoGTPases (Tzima, 2006; Boon *et al.*, 2010). Overexpression of dominant-negative mutants of Rac1 or RhoA in sparse endothelial monolayers results in impaired elongation and alignment after 4 h of flow (Wojciak-Stothard and Ridley, 2003). Of note, Rac1 is rapidly activated upon

This article was published online ahead of print in MBoC in Press (<http://www.molbiolcell.org/cgi/doi/10.1091/mbc.E16-06-0389>) on May 17, 2017.

The authors have no conflict of interest to disclose.

\*Address correspondence to: Jaap D. van Buul ([j.vanbuul@sanquin.nl](mailto:j.vanbuul@sanquin.nl)).

Abbreviations used: DORA, dimerization-optimized reporter for activation; ECs, endothelial cells; FRET, Förster resonance energy transfer; GEF, guanine-nucleotide exchange factor; HUVEC, human umbilical vein endothelial cells.

© 2017 Kroon *et al.* This article is distributed by The American Society for Cell Biology under license from the author(s). Two months after publication it is available to the public under an Attribution–Noncommercial–Share Alike 3.0 Unported Creative Commons License (<http://creativecommons.org/licenses/by-nc-sa/3.0>).

“ASCB®,” “The American Society for Cell Biology®,” and “Molecular Biology of the Cell®” are registered trademarks of The American Society for Cell Biology.

flow induction and localizes to the downstream side of the cell (Tzima *et al.*, 2002; Goldfinger *et al.*, 2008).

RhoGTPases are molecular switches that cycle between a GTP-bound, active state and a GDP-bound, inactive state (Etienne-Manneville and Hall, 2002). Key regulators in activating GTPases are guanine nucleotide exchange factors (GEFs; Rossman *et al.*, 2005). Of interest, the GEFs Tiam1 and Vav2 have been shown to be involved in the rapid onset of Rac1 activation upon flow (Liu *et al.*, 2013). Despite this, it is not known whether Rac1 activity or its polarized distribution is required for long-term flow-induced EC alignment.

Using a Förster resonance energy transfer (FRET)-based, dimerization-optimized reporters for activation (DORA) Rac1 biosensor, we found that Rac1 is not only continuously activated during long-term flow, but also that, in its active form, it localizes to the downstream side of the cell. Additional data show that the RhoGEF Trio functions as a scaffold protein rather than a GEF for keeping active Rac1 polarized in the presence of long-term flow conditions.

## RESULTS

### Long-term flow induces polarized Rac1 activity and stable junctions

The small GTPase Rac1 is activated and distributed to the downstream side of the EC upon short-term flow induction (Tzima *et al.*, 2002; Liu *et al.*, 2013). It is not known whether polarized Rac1 activity is maintained during long-term flow conditions. To address this, we examined the spatial and temporal activation of Rac1 under long-term laminar flow conditions: 12 h at 10 dynes/cm<sup>2</sup>. For this, we transfected ECs with a FRET-based DORA Rac1 biosensor (Timmerman *et al.*, 2015), grew them to confluency in specialized flow chambers, and applied flow. FRET-based ratiometric imaging showed rapid activation of Rac1 at the downstream side of the cell after 30 min of flow (Figure 1A). Although Rac1 activity showed a small decline at 1–2 h of flow, its activity level remained high for the duration of the experiment (Figure 1A). ECs kept under static conditions for the same period of time did not show any increase in Rac1 activity (Figure 1A and Supplemental Video S1). When measuring Rac1 activity biochemically using a G-LISA approach, we found similar kinetics (Figure 1B). Of interest, when analyzing the activity of Rac1 at specific locations, we found polarized Rac1 activity at the downstream side of the ECs to be increased significantly compared with the upstream side during longer periods of flow (Figure 1C). To study the importance of active Rac1 on the functional consequence of long-term flow conditions, that is, EC alignment, we treated ECs with the pharmacological inhibitor EHT1864 against Rac1 activity (Shutes *et al.*, 2007) and quantified EC alignment as described in *Materials and Methods*. Inhibition of Rac1 resulted in a failure of ECs to align under long-term flow conditions, indicating that Rac1 activation is crucial for flow-induced alignment of ECs (Figure 1D). In addition, long-term flow induced a phenotypic change in the morphology of the EC–cell junctions from an irregular shape toward a more linearized morphology, quantified by measuring the linearity of VE-cadherin between two junction points (Figure 1E; Timmerman *et al.*, 2015). Recently we showed that linear VE-cadherin-based junctions resulted in more stable junctions with increased barrier function (Timmerman *et al.*, 2015). To study whether flow-induced linearization of EC junctions also functionally promotes the barrier function of EC monolayers, we used electrical cell–substrate impedance sensing (ECIS) under flow technology. The data showed that that laminar flow at 10 dynes/cm<sup>2</sup> gradually increased the endothelial resistance in time, whereas ECs kept under static conditions did not show this increase (Figure 1F). These data show that long-term

flow induces Rac1-dependent alignment and drives active Rac1 to the downstream side of the EC. Moreover, long-term flow promotes the endothelial barrier function.

### The Rho-GEF Trio is required for flow-induced cell alignment

Activation of Rac1 is mediated by specific GEFs that catalyze the exchange from GDP to GTP. We recently reported that the RhoGEF Trio is responsible for local Rac1 activity to stabilize linear junctions (Timmerman *et al.*, 2015). To address whether Trio is required for flow-induced alignment, we depleted Trio in ECs using short hairpin RNA (shRNA) and studied long-term flow-induced alignment. We found that ECs lacking Trio failed to align in response to the flow within the 12-h imaging window (Figure 2A). Detailed analysis of the phenotypic changes using fluorescence microscopy showed impaired linearization of the EC junctions in Trio-deficient cells in response to the flow (Figure 2B). Moreover, ECs silenced for Trio failed to promote the endothelial barrier function upon 12 h of flow compared with untreated ECs (Figure 2C). Inspection of the endothelial monolayer morphology with differential interference contrast microscopy found that shCtrl-treated ECs showed the alignment phenotype upon flow, whereas Trio-deficient ECs did not (Supplemental Figure S1A). These data support a prominent role for Trio in regulating long-term flow-induced cell alignment and junctional integrity under flow.

### Trio N-terminus is required for flow-induced EC alignment

To elucidate how Trio regulates flow-induced EC alignment, we used different Trio constructs to rescue flow-induced alignment in Trio-deficient ECs. Trio is a 350-kDa protein with three catalytic domains and nine spectrin repeats at the N-terminus and also includes a Sec 14 lipid interactive domain. A schematic overview of the different Trio deletion mutants used in this study is given in Figure 3A. For these rescue experiments, we used a shRNA against Trio that was directed to the C-terminal SH3-domain region, as described previously (Timmerman *et al.*, 2015). To our surprise, only the TrioN mutant and not the GEF1 or GEF2 mutant (Blangy *et al.*, 2000; van Rijssel *et al.*, 2012a) rescued alignment upon flow in Trio-deficient ECs (Figure 3B). Expression of TrioN also rescued flow-induced electrical resistance in Trio-deficient ECs (Figure 3C). Figure 3D shows efficient Trio depletion and overexpression of green fluorescent protein (GFP)-TrioN in these cells. Together these experiments indicate that domains other than the Rac1/RhoG-activating GEF1 domain in the N-terminus of Trio can rescue Trio-mediated long-term flow-induced cell alignment.

### Trio-GEF1 activity is not required for flow-induced alignment

To further elucidate the role of Trio in flow-induced cell alignment, we used a selective inhibitor for the TrioGEF1 domain, ITX3 (Bouquier *et al.*, 2009; van Rijssel *et al.*, 2012b). In line with the rescue experiments, ITX3-treated ECs aligned normally upon long-term flow, supporting the rescue experiments from Figure 3B and showing that there is no need for TrioGEF1 activity for flow-induced EC alignment (Figure 4A). We observed irregular and reduced linearization of EC–cell junction, underscoring our previous findings that TrioGEF1 activity regulates stabilization of cell–cell junction integrity (Timmerman *et al.*, 2015; Figure 4A). To exclude fully that the activity of the TrioGEF1 domain is involved in Trio-mediated long-term flow-induced alignment, we used a GEF catalytic-dead mutant of Trio (N1406A/D1407A). When this mutant was expressed in HEK293 T-cells, it was unable to activate its downstream targets, Rac1 and RhoG, as measured with classical biochemical CRIB and

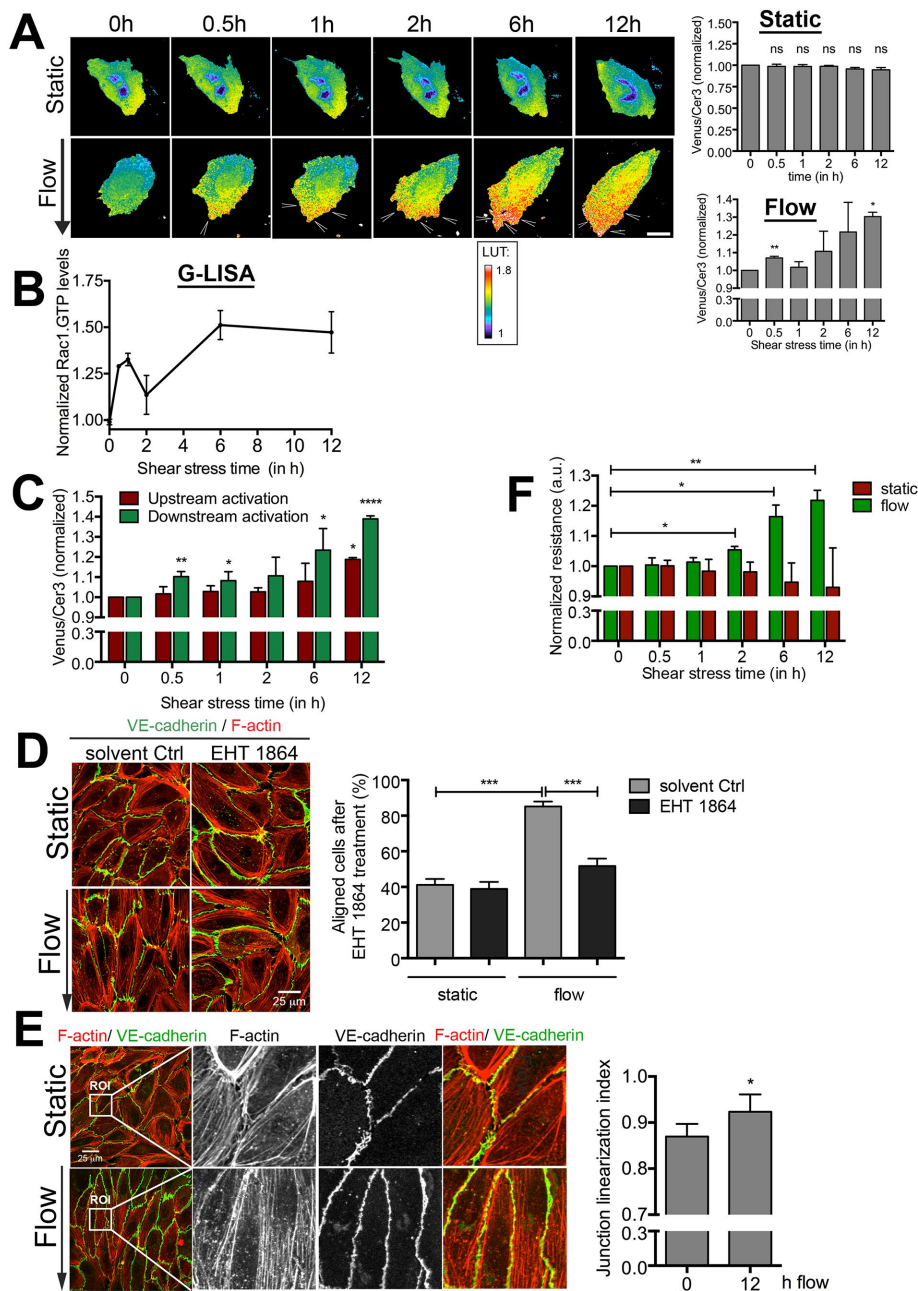


**FIGURE 1: Active Rac1 is required for flow-induced alignment.** (A) Left, time-lapse Venus/Cer3 ratio images of the Rac1 DORA biosensor simultaneously recorded with an epifluorescence microscope, showing spatiotemporal Rac1 activation under static conditions or upon flow (arrowheads; total 12 h; arrow shows direction of flow; flow speed, 10 dynes/cm<sup>2</sup>). Direction of flow is from top to bottom. Bar, 25  $\mu$ m. Calibration bar (LUT) shows Rac1 activation (red) relative to basal Rac1 activity (blue). Right, activation ratio of the Rac1 biosensor in time. Top, static conditions; bottom, flow conditions. Data are mean of three independent experiments  $\pm$  SEM. Significance compared with 0 h. \* $p$  < 0.05, \*\* $p$  < 0.01. (B) Rac1 activity measured with G-LISA at different shear stress times (30 min and 1, 2, 6, and 12 h). \* $p$  < 0.05. (C) FRET ratio measured in upstream (red) and downstream (green) sides of the cell upon the induction of flow. Rac1 activity was particularly detected at the downstream side. Data are mean of three independent experiments  $\pm$  SEM. Significance compared with 0 h. \* $p$  < 0.05; \*\* $p$  < 0.01; \*\*\*\* $p$  < 0.001. (D) Left, inhibition of Rac1 activity by EHT 1864 blocks alignment under flow, whereas solvent control-treated ECs are aligned in the direction of flow. Note that the inhibitor was present throughout the experiment due to the closed system used for long-term flow experiments. Right, percentage of aligned cells under static and flow conditions for both EHT 1864-treated and solvent-treated Ctrl ECs. ECs orientated with a 0–45° angle are quantified as being aligned. Data are mean of three independent experiments  $\pm$  SEM. \*\*\* $p$  < 0.001. Bar, 25  $\mu$ m. (E) Left, long-term flow results in linearized VE-cadherin-based cell–cell junctions. F-actin in red and

glutathione S-transferase (GST)–ELMO pull-down assays (Figure 4B; van Rijssel et al., 2012a). When expressing this mutant, which was insensitive for the shTrio used, in Trio-deficient ECs, we found that it rescued the defect in the flow-induced alignment phenotype of Trio-deficient ECs (Figure 4C). To study whether flow-induced Rac1 activity was unaffected in the Trio-deficient ECs, we used the aforementioned G-LISA technique and measured Rac1 activity in small cell lysate volumes. We found that flow activated Rac1 in Trio-deficient ECs to the same extent as in the shCtrl-treated ECs (Figure 4D). Trio-deficient cells, however, did not show alignment upon flow (Supplemental Figure S1B). On the basis of these findings, we conclude that flow-induced activity of Rac1 is independent of TrioGEF1 activity.

### Flow immobilizes Trio at cell–cell junctions

We next analyzed where Trio localizes upon the induction of flow. Owing to a lack of proper antibodies to stain endogenous Trio, we used GFP-Trio full-length (FL) constructs. GFP-TrioFL localized at EC junctions together with VE-cadherin (Figure 5A). Of interest, flow promoted colocalization between Trio and VE-cadherin at cell–cell junctions, as determined by the fluorescent pixel overlap ratio between GFP-Trio and VE-cadherin (Figure 5, A and B). To study whether flow influences the dynamics of Trio at cell–cell junctional regions, we performed fluorescent recovery after photobleaching (FRAP) experiments. These experiments revealed that long-term flow increased the immobile fraction of GFP-TrioN at EC–cell junction areas, whereas the mobility of GFP-TrioN in the cytosol was unaltered (Figure 5C). Of importance, we did not measure any change in the mobility of VE-cadherin–GFP after exposure to flow compared with static conditions (Figure 5C). These data show

VE-cadherin in green. ROI, region of interest. Bar, 25  $\mu$ m. Right, junction linearization index. Per experiment, three fields of view were quantified for junction linearization after 12 h of 10 dynes/cm<sup>2</sup> compared with 12 h of static conditions. Data are mean of three independent experiments  $\pm$  SEM. \* $p$  < 0.05. (F) Resistance measurements using ECIS under long-term flow conditions show an increase in monolayer integrity under long-term flow conditions (10 dynes/cm<sup>2</sup>; green), whereas the resistance did not change under static (red) conditions. Data are mean of three independent experiments  $\pm$  SEM. \* $p$  < 0.05.

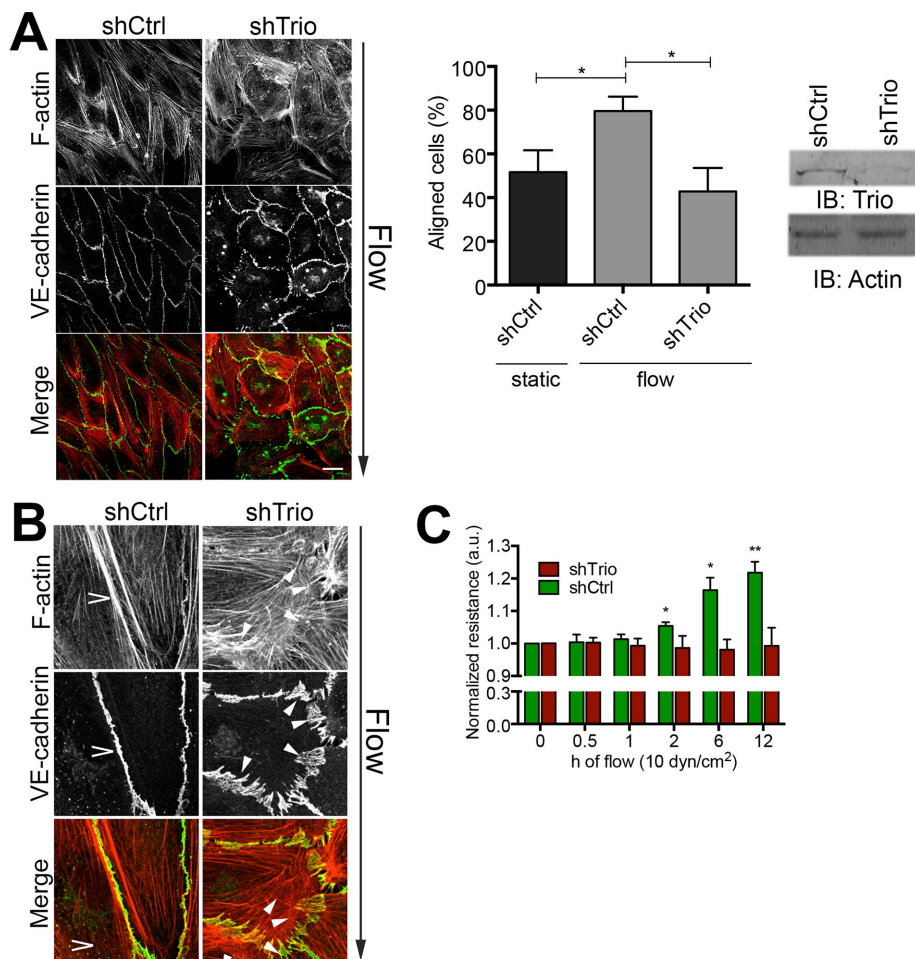


**FIGURE 2:** Trio silencing inhibits flow-induced EC alignment. (A) Left, HUVECs treated with Ctrl and Trio shRNA (shCtrl and shTrio) were applied to flow for 12 h. Direction of flow is from top to bottom. Trio-deficient ECs failed to align. Bar, 25  $\mu$ m. Middle, quantification of EC alignment upon flow vs. static conditions. Cells orientated between 0 and 45° are quantified as aligned. Data are mean of three independent experiments  $\pm$  SEM. \* $p < 0.05$ . Right, Trio depletion with shRNA analyzed by Western blotting; actin is used as loading control. (B) Magnification of EC–cell junctions. Flow induces linear junction (open arrowhead), marked by VE-cadherin in green and F-actin in red. Depletion of Trio (shTrio) results in unstable, zipper-like junctions (closed arrowheads). Bar, 25  $\mu$ m. (C) Resistance measurements using ECIS under flow conditions as indicated show that flow promotes EC resistance in time (green), whereas ECs depleted for Trio failed to increase flow-induced barrier resistance in time. Data are mean of three independent experiments  $\pm$  SEM. \* $p < 0.05$ ; \*\* $p < 0.01$ .

that long-term flow promotes Trio immobilization at EC–cell junction regions.

### Trio regulates flow-induced localization of active Rac1

Because the RacGEF domain of Trio is not directly involved in flow-induced cell alignment, we hypothesized that Trio targets the distribution of active Rac1 to the downstream side of the cell in response to long-term flow. To test this, we lentivirally transduced ECs with a previously characterized red fluorescent protein (RFP)-tagged shRNA-targeting Trio (Timmerman *et al.*, 2015) to visualize Trio-deficient ECs and subsequently transfected them with the DORA-based Rac1 biosensor (Figure 6A). Note that silencing Trio did not alter basal Rac1 activity levels (Van Rijssel *et al.* 2013; Timmerman *et al.*, 2015). Next we exposed the cells to flow for 12 h and recorded the activity and localization of Rac1. Strikingly, flow rapidly induced activation of Rac1 (30 min) in the Trio-deficient ECs, albeit

not significantly, followed by a decline and a second activation peak of Rac1 at later time points (Figure 6B and Supplemental Video S2). However, when analyzing the distribution of Rac1 activity within the EC, we found that there was no difference in Rac1 activation between the downstream and upstream areas (Figure 6C). Note that overall Rac1 activity after 12 h of flow was found to be somewhat lower in Trio-depleted ECs than in control ECs (Figure 1C). These data indicate that Trio regulates the localization rather than the activation of Rac1 upon long-term flow conditions in order to induce long-term flow-mediated EC alignment.

### DISCUSSION

In this study, we show that the RhoGEF Trio is required for proper EC alignment upon long-term flow conditions by keeping Rac1 activity polarized at the downstream side. We found that under these conditions, Trio serves as a scaffold protein rather than a functional GEF.

Our study shows that flow keeps Rac1 activity high at the downstream side of the ECs, allowing ECs to align. Because we also showed that ECs require the RhoGEF Trio for proper cell alignment and Trio is known to be an exchange factor for Rac1, we were surprised to find that the RacGEF activity of Trio was not required in this process. Instead, the adjacent N-terminal domain appear to be involved because a TrioN catalytic-dead mutant could at least partially rescue cell alignment in Trio-deficient ECs. In particular, the spectrin repeats—three-helix bundle structures that can be found in many proteins—can unfold after application of mechanical stress and therefore have the ability to interact with other proteins (Djinovic-Carugo *et al.*, 2002; Law *et al.*, 2003). This makes Trio, besides being a GEF, also a potential mechanosensing protein with scaffolding characteristics that may be involved in recruiting protein complexes to

specific locations in the cell—for instance, as described here, upon long-term flow conditions.

Additional experiments implicate Trio as acting on EC junction stability. Using VE-cadherin as an endothelial junction marker, we showed that VE-cadherin-based junctions appear to stabilize upon flow in a Trio-dependent manner. Moreover, flow immobilized Trio at junctional regions and promoted colocalization of VE-cadherin and Trio. Because VE-cadherin is one of the main mechanotransducers in ECs to translate changes in flow conditions (Tzima *et al.*, 2005) and we previously showed that Trio and VE-cadherin can physically interact with each other (Timmerman *et al.*, 2015), we hypothesize that flow may induce Trio/VE-cadherin interaction. Unfortunately, due to limited cell numbers in our flow setup, we were unable to perform these biochemical immunoprecipitation experiments. Nevertheless, it is tempting to speculate that Trio collaborates with the VE-cadherin/PECAM/VEGFR2 complex at

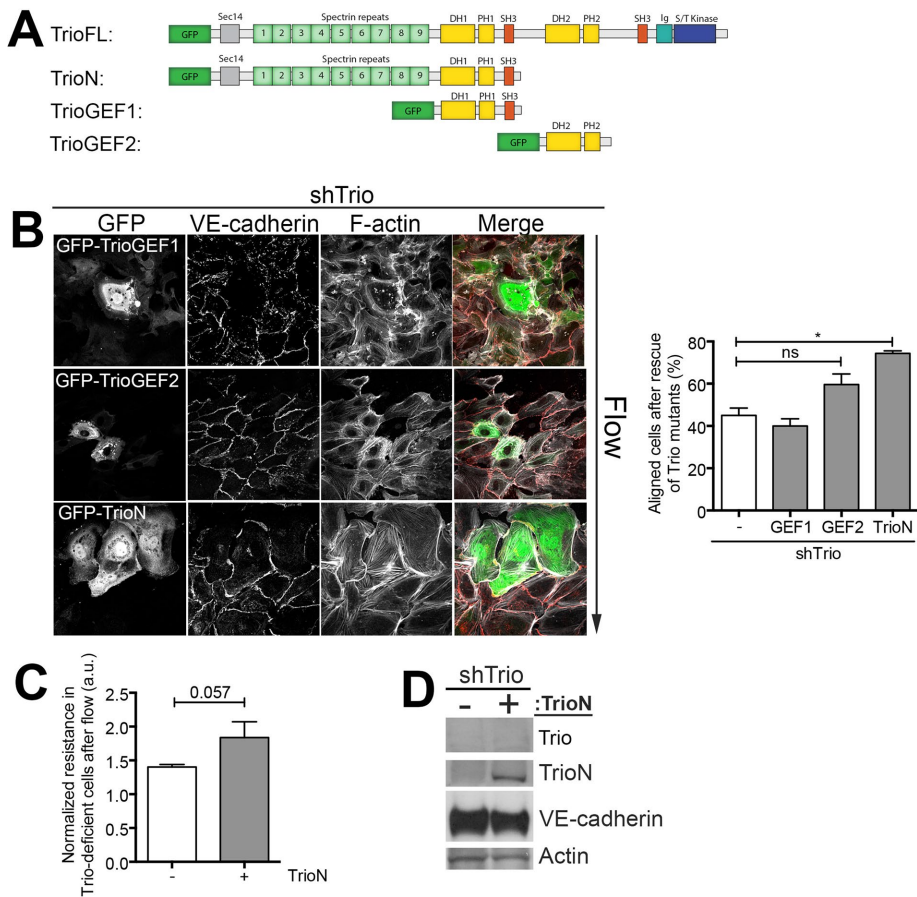


**FIGURE 3:** The N-terminal part of Trio rescues alignment and loss in resistance in Trio-deficient ECs. (A) Schematic overview of shRNA-insensitive GFP-tagged mutants GFP-TrioN, GFP-TrioGEF1, and GFP-TrioGEF2. Trio consists of three catalytic domains. GEF domain 1 activates Rac1 and RhoG, and GEF domain 2 activates RhoA and a serine/threonine kinase domain at the C-terminus. (B) Left, immunofluorescence staining of shTrio-treated ECs and overexpression of GFP-TrioGEF1, GFP-TrioGEF2, and GFP-TrioN and were subjected to 12 h of flow. Direction of flow is from top to bottom. GFP is shown in green, VE-cadherin in red, and F-actin in white. Right, quantification of aligned cells upon rescue of Trio expression indicates that TrioN expression rescues flow-induced alignment. Data are mean of three independent experiments  $\pm$  SEM.  $*p < 0.05$ . (C) ECIS under flow was used to measure the EC monolayer resistance in control and Trio-knockdown conditions. Normalized resistance after 12 h of flow. Data are mean of three independent experiments  $\pm$  SEM.  $*p < 0.05$ . (D) Western blot analysis confirmed the knockdown of Trio and subsequent overexpression of GFP-TrioN. VE-cadherin expression is not affected; actin is shown as loading control.

cell-cell junctions to regulate long-term flow-induced alignment by acting as a mechanosensing protein that would locally scaffold an as-yet-undefined Rac-activating protein complex.

Several years ago, a VE-cadherin-Par3-p67phox complex was identified that initiated flow-induced polarization in ECs by targeting Rac1 activity (Liu *et al.*, 2013). As with Trio, the RhoGEF Tiam1 was found to act as a scaffold rather than an exchange activator in flow-induced polarity (Liu *et al.*, 2013). This complex was assembled relatively early upon the onset of flow. In line with these results, our data show that in Trio-deficient cells, for short-term flow, that is, 30 min, Rac1 activity is increased and localized at the downstream side. For long-term flow conditions, Trio seems to play a more crucial role in maintaining this polarized Rac1 activation, resulting in increased cell alignment. These data indicate that short- and long-term flow conditions can have different effects on signaling complexes on the same cells, potentially with different phenotypic outcomes.

A question remains: what is the GEF responsible for activating Rac1? We looked into the role of Vav2 in EC alignment and performed additional experiments. ECs were depleted for Vav2 using small interfering RNAs and applied to shear for 12 h. To our surprise, the cells aligned normally upon addition of flow. Liu *et al.* (2013) showed that Vav2 is the responsible GEF for Rac1 activation upon flow at early time points, that is, 30 min and 1 h. However, it was not investigated whether this results in impaired alignment. Our data indicate that Vav2 is not required for ECs to align upon long-term flow conditions (unpublished data). Because Vav2 did not show any effect on cell alignment after 12 h of flow, we postulate that more GEFs or possibly compensatory mechanisms may be at play. In conclusion, Trio is required for long-term flow-induced continuous polarization of ECs by keeping Rac1 activity at the downstream side by acting as a scaffolding protein rather than a RhoGEF. Thus Trio may potentially scaffold other, as-yet-undefined RhoGEFs to locally promote GTP exchange on Rac1. Our findings may help to identify novel targets in order to regulate EC polarization in disturbed flow areas and thereby promote cell alignment and prevent vascular inflammation.

## MATERIALS AND METHODS

### Antibodies and reagents

Trio (clone D-20) and VE-cadherin (F8) antibodies were from Santa Cruz Biotechnologies (Dallas, TX). Actin (clone AC-40) monoclonal antibody was purchased from Sigma-Aldrich (Zwijndrecht, Netherlands). Mouse polyclonal Trio antibody was from Abnova (Heidelberg, Germany). Secondary horseradish peroxidase (HRP)-conjugated goat anti-mouse, goat anti-rabbit, and rabbit anti-goat antibodies were purchased from Dako (Heverlee, Belgium). Directly labeled VE-cadherin was purchased from BD (clone 55-7H1). To visualize F-actin filaments, differently fluorescently labeled phalloidin was used (Invitrogen, Bleiswijk, Netherlands). Finally, Hoechst 33258 was used to visualize the nucleus. Secondary infrared labeled anti-mouse, anti-rabbit, and anti-goat antibodies used for visualization of proteins by means of Odyssey were from Westburg (Leusden, Netherlands).

### Cell culture and transfection

Primary human umbilical vein endothelial cells (HUVECs) were purchased from Lonza (Baltimore, MD) and maintained on fibronectin (30  $\mu$ g/ml; Sanquin Reagents, Amsterdam, Netherlands)-coated, tissue culture-treated culture flasks (TPP, Switzerland) or glass slides in EGM2-containing SingleQuots (Lonza). ECs were cultured up to passage four. HUVECs were subjected to shear stress for the indicated time periods. To inhibit TrioGEF1 activity, and thus Rac1 and

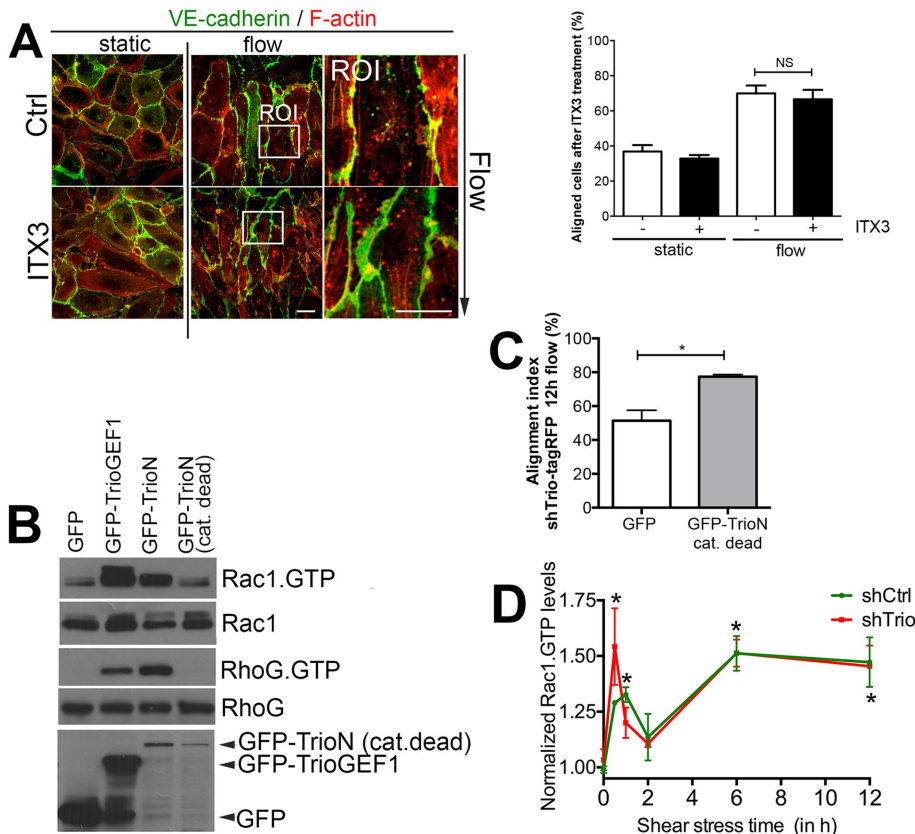


**FIGURE 4:** The activity of TrioGEF1 is not necessary for flow-induced alignment. (A) Left, TrioGEF1 activity was blocked by ITX3. Inhibition of GEF1 activity does not interfere with flow-induced alignment. VE-cadherin is shown in green and F-actin in red. ROI shows zoom of EC–cell junction region. Direction of flow is from top to bottom. Bar, 25  $\mu$ m. Right, quantification of EC alignment. Data are mean of three independent experiments  $\pm$  SEM. NS, not significant. (B) GFP-tagged Trio constructs were transfected in HEK293 cells and subjected to biochemical Rac1 and RhoG pull-down assays. GFP-TrioN-GEF N1406A/D1407A mutant (cat. dead) failed to induce Rac1 (GTP; top) and RhoG (GTP; third panel) activity, whereas GFP-TrioGEF1 and GFP-TrioN did. Second and fourth panels show Rac1 and RhoG protein expression as input controls. Bottom, expression of GFP-tagged constructs in cell lysates. (C) shTrio-tagRFP ECs were transfected with GFP-TrioN-N1406A/D1407A (cat. dead) and subjected to 12 h of flow. Rescue of Trio expression with GFP-TrioN catalytic-dead mutant rescued flow-induced alignment. Data are mean of three independent experiments  $\pm$  SEM. \* $p < 0.05$ . (D) Data obtained from Rac1 G-LISA experiments show that flow (measured at different time points as indicated) increases Rac1 activation (Rac1.GTP) in both control (shCtrl) and Trio-deficient (shTrio) cells. Significance is indicated time point compared with 0 h. \* $p < 0.05$ .

RhoG activity, cells were pretreated for 2 h with ITX3 (75  $\mu$ M; purchased from ChemBridge, San Diego, CA; Bouquier *et al.*, 2009) and then subjected to shear stress for different periods of time, as indicated. To specifically inhibit Rac1 activity, cells were pretreated with 12.5 mM EHT 1864 (Selleckchem, Munich, Germany) for 2 h, before applying shear stress. HUVECs were transfected with GFP-TrioFL via electroporation using the Neon transfection system (one pulse, 1350 V, 30 ms) according to manufacturer's protocol (Life Technologies, Bleiswijk, Netherlands). shRNA constructs targeting Trio, tagRFP-Trio shRNA, and a nonspecific control shRNA (shCtrl) were used to produce lentivirus in HEK 293T cells by using the third-generation packaging plasmids (Hope *et al.*, 1990; Dull *et al.*, 1998). The lentivirus-containing supernatant was harvested 2 and 3 d after transfection, filtered, and concentrated by using Lenti-X Concentrator (Clontech, Saint-Germain-en-Laye, France) according to the manufacturer's protocol.

Lentivirally transduced cells were used 3 d after transduction for further processing.

### FRET-based biosensor analysis

The DORA Rac1 FRET-based biosensor was a kind gift from Y. Wu (University of Connecticut Health Center, Farmington, CT). Development and characterization of the DORA single-chain Rac1 biosensor are described in more detail elsewhere (Timmerman *et al.*, 2015). Briefly, dimeric cereulean3 coupled to the Rac1 effector p21-activated protein kinase (PAK) is linked via ribosomal protein-based linker (L9H) with circular-permuted Venus coupled to Rac1. Before the experiment, cells were electroporated using the Neon transfection system (Life Technologies). In short, HUVECs were transfected with the Rac1-biosensor via electroporation (one pulse, 1300 V, 30 ms) and used 24 h posttransfection. A Zeiss Observer Z1 microscope equipped with a 40 $\times$ /numerical aperture 1.3 oil immersion objective, an HXP 120-V excitation light source, a Chroma 510 DCSP dichroic splitter, and two Hamamatsu ORCA-R2 digital charge-coupled device cameras were used for simultaneous monitoring of Cer3 and Venus emission. Zeiss Zen 2012 microscope software was used to control the system. Offline ratio analyses between Cer3 and Venus images were processed using the MBF ImageJ collection (Collins, 2007). Image stacks were background corrected, stacks were subsequently aligned, and a smooth filter to both image stacks was applied to improve image quality by noise reduction. An image threshold was applied exclusively to the Venus image stack, converting background pixels to "not a number (NaN)," eliminating artifacts in ratio image stemming from the background noise. Finally, the Venus/Cer3 ratio was calculated, with high activation shown in red/white and low activity in blue/black.

### Quantification of cell alignment

EC alignment was quantified by measuring the angle of a line drawn between the two most opposite points of the cell compared with the direction of the flow. If the angle was  $<45^\circ$ , the cell was quantified as aligned. If the angle was  $>45^\circ$  compared with the direction of the flow, cells were quantified as not aligned (Supplemental Figure S2).

### Quantification of junction linearization

EC cell–cell junctions were stained for VE-cadherin. The actual length of a VE-cadherin-positive junction was measured between two endpoints of the cell-to-cell junction. This number was divided by the length of the straight line drawn between the two same points. The outcome is a representation of the linearity of the endothelial VE-cadherin-based cell–cell junction, with maximum junction linearity index 1 indicating a linear junction.

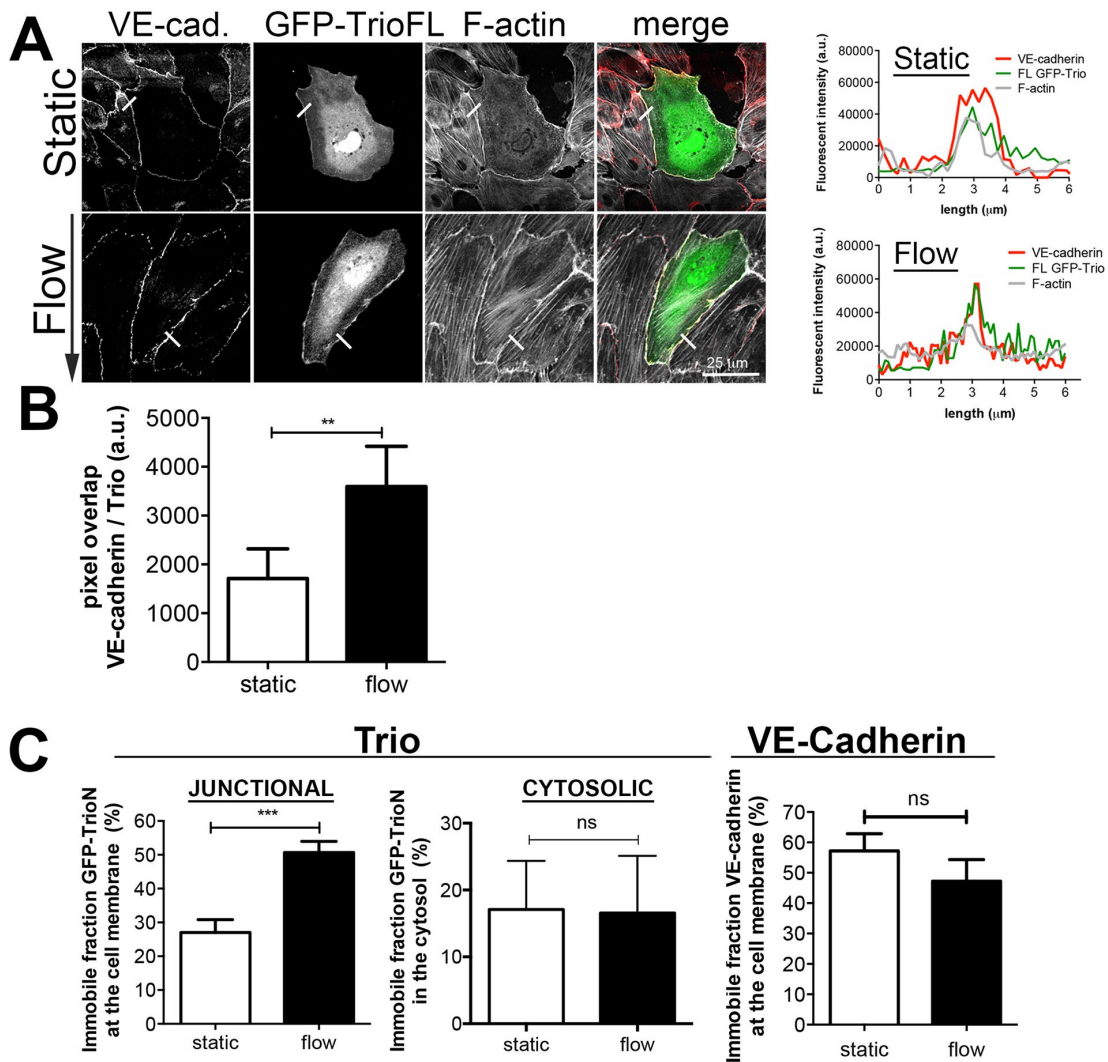


**FIGURE 5:** Flow promotes Trio immobilization at junction regions and Trio colocalization with VE-cadherin. (A) Left, ECs were transfected with GFP-TrioFL and subjected to flow (12 h) or left untreated. Flow induces colocalization of GFP-TrioFL (green) with VE-cadherin (white). Red, F-actin. Right, fluorescence intensity of the bar (6  $\mu\text{m}$  in length) on the main figure, showing increased colocalization between TrioFL (green) and VE-cadherin (red). Bar, 25  $\mu\text{m}$ . (B) Pixel overlap between VE-cadherin and GFP-TrioFL under static conditions or flow (12 h) conditions.  $**p < 0.01$ . (C) FRAP was performed on GFP-Trio under static or flow (12 h) conditions at junctional regions or cytosolic areas, as indicated. Flow increases the immobile fraction of Trio at junctions, whereas no difference was detected in the cytosol. VE-cadherin–GFP FRAP analysis showed no difference in mobility under static and flow conditions. Data are mean of three independent experiments  $\pm$  SEM.  $***p < 0.001$ . ns, not significant.

### Adenovirus production

GFP-TrioGEF1, GFP-TrioGEF2, and GFP-TrioN were obtained as previously described (van Rijssel *et al.*, 2012a). Briefly, adenovirus expressing GFP-TrioGEF1, GFP-TrioGEF2, and GFP-TrioN was produced by transfecting *PacI*-digested (Westburg, Leiden, Netherlands) constructs into HEK293T cells.

### Western blotting

Cells in IBIDI slides (IBIDI, Planegg, Germany) were washed three times with ice-cold phosphate-buffered saline (PBS) containing 1 mM  $\text{CaCl}_2$  and 0.5 mM  $\text{MgCl}_2$  and boiled in SDS-sample buffer containing 4%  $\beta$ -mercaptoethanol. Samples were analyzed by SDS–PAGE or 3–8% Tris-acetate gradient gels (Invitrogen), transferred to a 0.2- $\mu\text{m}$  nitrocellulose membrane (Whatman, Dassel, Germany), and blocked with blocking buffer containing 5% (wt/vol)

nonfat dry milk in Tris-buffered saline with Tween-20 (TBST). The nitrocellulose membrane was incubated with specific primary antibodies for 1 h at room temperature, followed by incubation with secondary HRP-conjugated antibodies for 1 h at room temperature. Among all of the incubation steps, the blots were washed at least three times with TBST for 10 min. Staining was visualized with enhanced chemiluminescence detection system (Pierce, Rockford, IL) or by infrared imaging using the Odyssey system (LI-COR Biosciences, Lincoln, NE).

### Immunofluorescence

Immunofluorescence-stained ECs were grown on fibronectin-coated IBIDI slides. After treatment, ECs were washed twice with room temperature PBS<sup>++</sup> (PBS supplemented with 1 mM  $\text{CaCl}_2$  and 0.5 mM  $\text{MgCl}_2$ ) and subsequently fixed in 3.7% (vol/vol) formaldehyde in

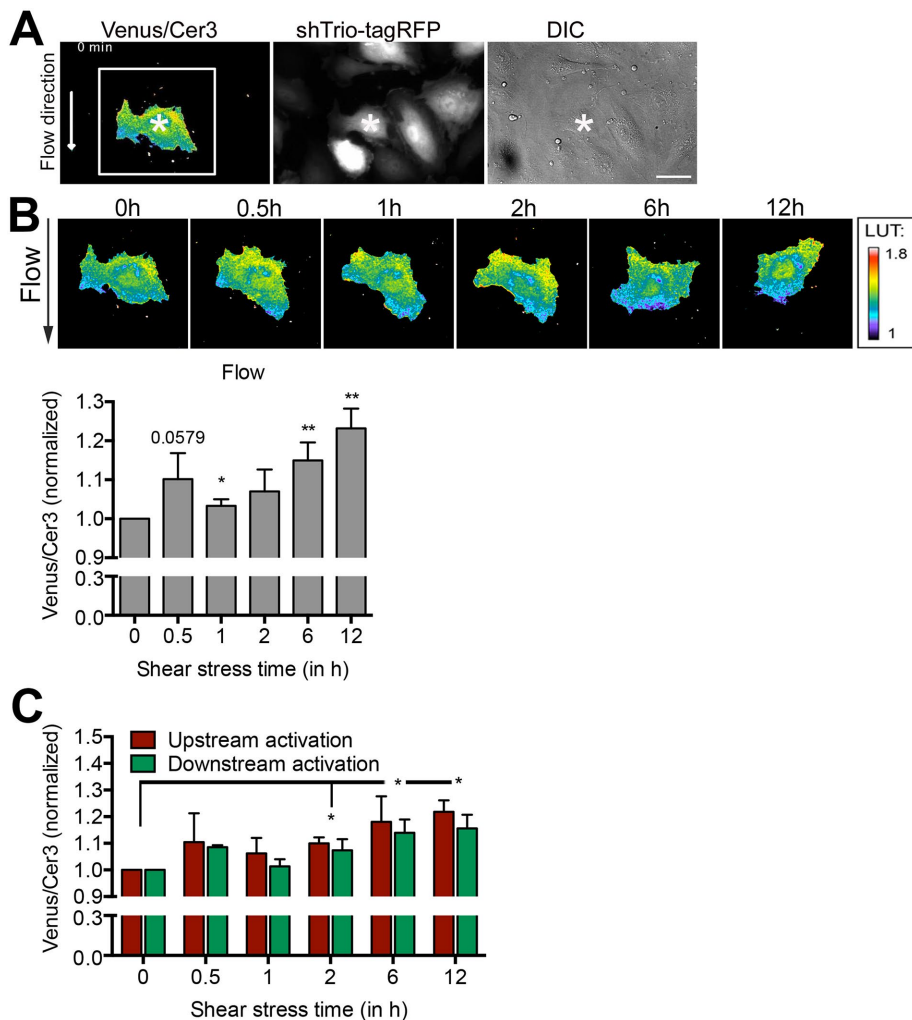


**FIGURE 6:** Trio regulates the localization of active Rac1. (A) HUVECs were first transduced with shRNA targeting Trio containing an RFP tag (shTrio-tagRFP) and subsequently transfected with the FRET-based DORA Rac1 biosensor. Right, differential interference contrast (DIC). Bar, 25  $\mu$ m. (B) Top, ECs were subsequently exposed to flow (12 h), and Rac1 activity and localization were monitored. Calibration bar (LUT) shows Rac1 activation (red) relative to basal Rac1 activity (blue). Bottom, quantification of ratiometric imaging analysis (Venus/Cer3) of the whole cell upon exposure to flow. Even in the absence of Trio, flow rapidly activates Rac1 at 30 min, followed by a decline and a second activation increase. \* $p < 0.05$ ; \*\* $p < 0.01$ . (C) Activation ratio of the Rac1 biosensor in time at the downstream (green) and upstream (red) sides of the EC side of the cell. No significance is calculated between downstream and upstream regions for Rac1 activation. However, overall Rac1 activity is increased significantly compared with 0-h time point. Data are mean of three independent experiments  $\pm$  SEM. \* $p < 0.05$ .

PBS<sup>++</sup> for 10 min. After fixation, cells were permeabilized in PBS plus 0.1% Triton-X100 for 10 min. Next cells were incubated with primary and secondary antibodies and, between each incubation, washed three times with PBS<sup>++</sup>. Finally, cells were kept in PBS<sup>++</sup> until imaging with a confocal laser-scanning microscope (LSM510 META; Carl Zeiss MicroImaging, Jena, Germany). FRAP experiments were performed using 50 iterations with 488-nm laser illumination at maximum power (25 mW). Fluorescence recovery was measured by time-lapse imaging. Prism 6 (GraphPad Software, La Jolla, CA) was used for statistical analysis and nonlinear regression. A single-exponential association was used for curve fitting:  $Y = Y^{\max}[1 - \exp(-KX)]$ , which starts at 0 and ascends to  $Y^{\max}$  with a rate constant  $K$ , where  $Y^{\max}$  represents the mobile fraction and  $K$  represents the time characteristic of the curve.

### Laminar pulsatile flow system

All cell cultures were kept in a humidified atmosphere of 95% air and 5% CO<sub>2</sub> at 37°C. Before the experiment, cells were seeded at semiconfluence in IBIDI VI microslides. At 4 h after seeding, the slide was connected to a peristaltic pump equipped with eight roller heads to decrease the pulse and a bubble trap (Technical University of Denmark, Kongens Lyngby, Denmark) to filter out air bubbles in the closed flow system. A surface area of 0.8 cm<sup>2</sup> was exposed to fluid shear stress generated by perfusing culture medium over the cells. The physiological shear stress in arteries, 10 dynes/cm<sup>2</sup>, was used for all experiments.

### Rac1 and RhoG pull-down assays

Classical biochemical pull-down assays were performed as described (van Rijssel et al., 2012a). Briefly, a confluent monolayer of HUVECs washed with ice-cold PBS<sup>++</sup> and subsequently lysed in 50 mM Tris, pH 7.4, 0.5 mM MgCl<sub>2</sub>, 500 mM NaCl, 1% (vol/vol) Triton X-100, 0.5% (wt/vol) deoxycholic acid, and 0.1% (wt/vol) SDS supplemented with protease inhibitors. Lysates were cleared at 14,000  $\times$  g for 5 min. GTP-bound RhoG was isolated by rotating supernatants for 30 min with 60–90  $\mu$ g of GST-ELMO (GST-fusion protein containing the full-length RhoG effector ELMO) conjugated to glutathione-Sepharose beads (GE Healthcare, Zeist, Netherlands). GTP-bound Rac1 was isolated with biotinylated Pak1-Crib peptide coupled to streptavidin agarose. Beads were washed four times in 50 mM Tris, pH 7.4, 0.5 mM MgCl<sub>2</sub>, 150 mM NaCl, 1% (vol/vol) Triton X-100, and protease inhibitors. Pull downs and lysates were immunoblotted with monoclonal RhoG and Rac1 antibodies.

### Electric cell-substrate impedance sensing under laminar flow

Endothelial monolayer integrity was determined by measuring the electrical resistance using ECIS. Flow chamber electrode arrays (8F10E; Applied Biophysics, Troy, NY) were pretreated with 10 mM L-cysteine (Sigma-Aldrich) for 15 min at 37°C, subsequently washed twice with 0.9% NaCl, and coated with fibronectin (Sanquin) in 0.9% NaCl for 1 h at 37°C. Cells were seeded at 200,000 cells/slide (2.5 cm<sup>2</sup>). Continuous resistance measurements were performed at 37°C at 5% CO<sub>2</sub> with the ECIS Z0 (Theta) system controller (Applied Biophysics). After formation of a stable monolayer, the cells were subjected to flow (10 dynes/cm<sup>2</sup>) for 12 h.

### Statistical analysis

For statistical analysis between experimental groups, the Student's *t* test was used. A two-sided  $p \leq 0.05$  was considered significant. Unless stated otherwise, a representative experiment out of at least three independent experiments is shown.

## ACKNOWLEDGMENTS

We thank P. L. Hordijk and A. E. Daniel for critically reading the manuscript. GFP-TrioFL was a kind gift of A. Debant (Macromolecular Biochemistry Research Center, Montpellier, France). We also thank D. Geerts (Erasmus University Medical Center, Rotterdam, Netherlands) for supplying the shRNAs, L. Hodgson (Albert Einstein College of Medicine, New York, NY) for the Trio mutant, and Yi Wu (UConn Health, Farmington, CT) for longstanding collaboration on the DORA sensors. J.D.v.B. is supported by Dutch Heart Foundation Grant 2005T039, J.K. by Dutch Heart Foundation Grant 2005T3901, and N.H. by Landsteiner Foundation for Blood Transfusion Research Fellowship Grant 1028.

## REFERENCES

- Ballermann BJ, Dardik A, Eng E, Liu A (1998). Shear stress and the endothelium. *Kidney Int Suppl* 67, S100–S108.
- Blangy A, Vignal E, Schmidt S, Debant A, Gauthier-Rouviere C, Fort P (2000). TrioGEF1 controls Rac- and Cdc42-dependent cell structures through the direct activation of rhoG. *J Cell Sci* 113, 729–739.
- Boon RA, Leyen TA, Fontijn RD, Fledderus JO, Baggen JM, Volger OL, van Nieuw Amerongen GP, Horrevoets AJ (2010). KLF2-induced actin shear fibers control both alignment to flow and JNK signaling in vascular endothelium. *Blood* 115, 2533–2542.
- Bouquier N, Vignal E, Charrasse S, Weill M, Schmidt S, Leonetti JP, Blangy A, Fort P (2009). A cell active chemical GEF inhibitor selectively targets the Trio/RhoG/Rac1 signaling pathway. *Chem Biol* 16, 657–666.
- Chappell DC, Varner SE, Nerem RM, Medford RM, Alexander RW (1998). Oscillatory shear stress stimulates adhesion molecule expression in cultured human endothelium. *Circ Res* 82, 532–539.
- Chiu JJ, Chien S (2011). Effects of disturbed flow on vascular endothelium: pathophysiological basis and clinical perspectives. *Physiol Rev* 91, 327–387.
- Collins TJ (2007). ImageJ for microscopy. *Biotechniques* 43(1 Suppl), 25–30.
- Djinovic-Carugo K, Gautel M, Ylänne J, Young P (2002). The spectrin repeat: a structural platform for cytoskeletal protein assemblies. *FEBS Lett* 513, 119–123.
- Dull T, Zufferey R, Kelly M, Mandel RJ, Nguyen M, Trono D, Naldini L (1998). A third-generation lentivirus vector with a conditional packaging system. *J Virol* 72, 8463–8471.
- Etienne-Manneville S, Hall A (2002). Rho GTPases in cell biology. *Nature* 420, 629–635.
- Galie PA, Nguyen DH, Choi CK, Cohen DM, Janmey PA, Chen CS (2014). Fluid shear stress threshold regulates angiogenic sprouting. *Proc Natl Acad Sci USA* 111, 7968–7973.
- Goldfinger LE, Tzima E, Stockton R, Kiosses WB, Kinbara K, Tkachenko E, Gutierrez E, Groisman A, Nguyen P, Chien S, Ginsberg MH (2008). Localized alpha4 integrin phosphorylation directs shear stress-induced endothelial cell alignment. *Circ Res* 103, 177–185.
- Hahn C, Schwartz MA (2009). Mechanotransduction in vascular physiology and atherogenesis. *Nat Rev Mol Cell Biol* 10, 53–62.
- Hoger JH, Ilyin VI, Forsyth S, Hoger A (2002). Shear stress regulates the endothelial Kir2.1 ion channel. *Proc Natl Acad Sci USA* 99, 7780–7785.
- Hope TJ, McDonald D, Huang XJ, Low J, Parslow TG (1990). Mutational analysis of the human immunodeficiency virus type 1 Rev transactivator: essential residues near the amino terminus. *J Virol* 64, 5360–5366.
- Law R, Carl P, Harper S, Dalhaimer P, Speicher DW, Discher DE (2003). Cooperativity in forced unfolding of tandem spectrin repeats. *Biophys J* 84, 533–544.
- Liu Y, Collins C, Kiosses WB, Murray AM, Joshi M, Shepherd TR, Fuentes EJ, Tzima E (2013). A novel pathway spatiotemporally activates Rac1 and redox signaling in response to fluid shear stress. *J Cell Biol* 201, 863–873.
- Malek AM, Alper SL, Izumo S (1999). Hemodynamic shear stress and its role in atherosclerosis. *J Am Med Assoc* 282, 2035–2042.
- Pan S (2009). Molecular mechanisms responsible for the atheroprotective effects of laminar shear stress. *Antioxid Redox Signal* 11, 1669–1682.
- Rossman KL, Der CJ, Sondek J (2005). GEF means go: turning on RHO GTPases with guanine nucleotide-exchange factors. *Nat Rev Mol Cell Biol* 6, 167–180.
- Shutes A, Onesto C, Picard V, Leblond B, Schweighoffer F, Der CJ (2007). Specificity and mechanism of action of EHT 1864, a novel small molecule inhibitor of Rac family small GTPases. *J Biol Chem* 282, 35666–35678.
- Timmerman I, Heemskerk N, Kroon J, Schaefer A, van Rijssel J, Hoogenboezem M, van Unen J, Goedhart J, Gadella TW Jr, Yin T, et al. (2015). A local VE-cadherin/Trio-based signaling complex stabilizes endothelial junctions through Rac1. *J Cell Sci* 128, 3041–3054.
- Tzima E (2006). Role of small GTPases in endothelial cytoskeletal dynamics and the shear stress response. *Circ Res* 98, 176–185.
- Tzima E, del Pozo MA, Kiosses WB, Mohamed SA, Li S, Chien S, Schwartz MA (2002). Activation of Rac1 by shear stress in endothelial cells mediates both cytoskeletal reorganization and effects on gene expression. *EMBO J* 21, 6791–6800.
- Tzima E, Irani-Tehrani M, Kiosses WB, Dejana E, Schultz DA, Engelhardt B, Cao G, DeLisser H, Schwartz MA (2005). A mechanosensory complex that mediates the endothelial cell response to fluid shear stress. *Nature* 437, 426–431.
- van der Heiden K, Hierck BP, Krams R, de Crom R, Cheng C, Baiker M, Pourquie MJ, Alkemade FE, DeRuiter MC, Gittenberger-de Groot AC, Poelmann RE (2008). Endothelial primary cilia in areas of disturbed flow are at the base of atherosclerosis. *Atherosclerosis* 196, 542–550.
- van Rijssel J, Hoogenboezem M, Wester L, Hordijk PL, van Buul JD (2012a). The N-terminal DH-PH domain of Trio induces cell spreading and migration by regulating lamellipodia dynamics in a Rac1-dependent fashion. *PLoS One* 7, e29912.
- van Rijssel J, Kroon J, Hoogenboezem M, van Alphen FP, de Jong RJ, Kostadinova E, Geerts D, Hordijk PL, van Buul JD (2012b). The Rho-GEF Trio controls leukocyte transendothelial migration by promoting docking structure formation. *Mol Biol Cell* 23, 2831–2844.
- Van Rijssel J, Timmerman I, Van Alphen FP, Hoogenboezem M, Korchynskyi O, Geerts D, Geissler J, Reedquist KA, Niessen HW, Van Buul JD (2013). The Rho-GEF Trio regulates a novel pro-inflammatory pathway through the transcription factor Ets2. *Biol Open* 2, 569–579.
- Wojciak-Stothard B, Ridley AJ (2003). Shear stress-induced endothelial cell polarization is mediated by Rho and Rac but not Cdc42 or PI 3-kinases. *J Cell Biol* 161, 429–439.